



Research article

Clinical implication of radiographic scores in acute Middle East respiratory syndrome coronavirus pneumonia: Report from a single tertiary-referral center of South Korea



Min Jae Cha^{a,1}, Myung Jin Chung^{a,*}, Kyunga Kim^{b,c}, Kyung Soo Lee^a, Tae Jung Kim^a,
Tae Sung Kim^a

^a Department of Radiology and Center for Imaging Science, Samsung Medical Center, Sungkyunkwan University School of Medicine, Seoul 06351, Republic of Korea

^b Statistics and Data Center, Research Institute for Future Medicine, Samsung Medical Center, Seoul 06351, Republic of Korea

^c Department of Digital Health, SAIHST, Sungkyunkwan University, Seoul 06351, Republic of Korea

ARTICLE INFO

Keywords:

Middle East respiratory syndrome coronavirus (MERS-CoV)
Chest radiographic score
Chest radiograph
Prognostic indicator

ABSTRACT

The aim of this study is to determine the earliest cutoff of radiographic score as a potential prognostic indicator of fatal outcomes in patients with acute Middle East respiratory syndrome coronavirus (MERS-CoV) pneumonia. The institutional review board approved this retrospective study. Serial chest radiographies (CXRs) were obtained from viral exposure until death or discharge in 35 patients with laboratory confirmed MERS-CoV infection. Radiographic scores were calculated by multiplying a four-point scale of involved lung area and three-point scale of abnormal opacification, in each of the six lung zones. Receiver operating characteristics (ROC) analyses were performed to identify optimal day and radiographic score for the prediction of respiratory distress, and univariate and multivariate logistic regression analyses were performed to assess significant predictive factors for intubation or tracheostomy. Among 35 patients (22 men, 13 women; median age: 48 years), 25 demonstrated abnormal opacity on CXR (MERS pneumonia), whereas no abnormality was detected in 10 patients (MERS upper respiratory tract infection). Seven patients required ventilator support (intubation group) and three of them eventually expired. The average incubation period was 5.4 days (standard deviation, \pm 2.8; range, 2–11). Patients in the intubation group had a higher incidence of diffuse lung involvement, higher radiographic scores, and fibrosing sequela on follow up study compared with those in the non-intubation group. However, patients' age and comorbidity did not differ significantly between the two groups. The ROC analysis revealed an area under curve of 0.726 for the radiographic score on day 10 with an optimal cutoff score of 10 for prediction of intubation, with a sensitivity of 71% and specificity of 67%. Our study suggest that MERS patients with radiographic score > 10 on day 10 from viral exposure require aggressive therapy with careful surveillance and follow-up evaluation.

1. Introduction

Middle East respiratory syndrome (MERS) is an acute viral respiratory disease, caused by a novel virus called MERS coronavirus (MERS-CoV) [1,2]. Since the first reported case of MERS in Saudi Arabia in 2012, 1888 laboratory-confirmed cases of infection with MERS-CoV, resulting in 670 deaths across 27 countries, have been reported to the World Health Organization [3]. The first case of MERS in

Korea reported on May 20, 2015, was that of an individual who had developed the disease after traveling to the Middle East countries. Subsequently, this case led to the largest transmission cluster of MERS outside the Arabian Peninsula, resulting in 186 confirmed MERS cases in Korea [4]. Among these 186 cases, 36 were treated in our institution.

Imaging plays a crucial role in making a diagnosis and monitoring disease progress, and chest radiography (CXR) remains the most commonly used imaging modality. Because MERS can be transmitted

Abbreviations: MERS, Middle East respiratory syndrome; CoV, coronavirus; CXR, chest radiography; CT, computed tomography; ER, emergency room; ROC, receiver operating characteristic; URI, upper respiratory tract infection; AUC, area under the ROC curve

* Corresponding author at: Department of Radiology, Samsung Medical Center, Sungkyunkwan University School of Medicine, 50 Ilwon-Dong, Kangnam-Ku, Seoul 06351, Republic of Korea.

E-mail address: mj1.chung@samsung.com (M.J. Chung).

¹ Current address: Department of Radiology, Chung-Ang university hospital, Chung-Ang University College of Medicine, Seoul 06973, Republic of Korea.

<https://doi.org/10.1016/j.ejrad.2018.09.008>

Received 19 April 2018; Received in revised form 12 July 2018; Accepted 10 September 2018

0720-048X/© 2018 Published by Elsevier B.V.

through direct or indirect exposure to MERS-CoV, infection control in health care facilities is a critical issue [5–9]. Patients diagnosed with MERS should be moved to an institutional isolation care unit and personal protective equipment is mandatory for health care workers who handle these patients. Thus, CXR would play a pivotal role in the evaluation of patients with several infectious diseases, including MERS, because it is rapid and easily accessible, compared with computed tomography (CT). Indeed, we relied on the findings of sequential CXR while managing the 36 patients with MERS-CoV infection in clinical practice. However, there is still limited information about the prognostic implication of CXR findings in patients with MERS. Thus, the aim of this study was two-fold. First, we were to describe the serial radiographic characteristics of MERS-CoV pneumonia by analyzing radiographic scores. Second, we tried to identify the earliest cutoff value of radiographic score, which can be considered as a potential prognostic indicator of fatal outcomes in patients with MERS-CoV pneumonia.

2. Materials and methods

The institutional review board approved the study (IRB 2015-07-195), and informed consent was waived for the use of patients' medical and imaging data.

2.1. Study population and exposure

On May 27, 2015, a 35-year-old Korean man visited the emergency room (ER) of our institution with fever, productive cough, and dyspnea. After 2 days (May 29), he reported that he had met another patient with MERS approximately 10 days ago, at a different hospital. The patient was immediately transferred to an isolation care unit. The MERS-CoV infection was confirmed by a sputum assay on May 30. During his stay in the ER, numerous individuals were in contact with him directly or indirectly. Individuals with a possibility of exposure to this virus were quarantined and laboratory tests were conducted if symptoms were noted during the observational period. Consequently, 81 cases of MERS-CoV infection resulting from the exposure at the ER were confirmed, resulting in a total of 90 cases of MERS-CoV infection diagnosed at our institution [8]. Among the 90 patients, 36 were hospitalized in the isolation care unit of our institution. One patient with underlying stage-four lymphoma was not included in this study, as this condition could adversely affect the prognosis. Thus, 35 patients with laboratory-confirmed MERS were included.

We identified the exact time of exposure, symptom onset, and laboratory-diagnosis of MERS in every patient. In addition, all data, including age, sex, premorbid conditions, symptoms, laboratory findings, clinical course and survival outcome were collected from patient electronic medical records. The patients were then subdivided into two groups: patients who required intubation or tracheostomy (intubation group) and those who recovered without respiratory distress (non-intubation group).

2.2. Diagnosis of MERS-CoV infection

All of the diagnoses had been confirmed with real-time reverse-transcription polymerase chain reaction analysis of lower respiratory tract specimens, including sputum and endotracheal aspirates [10]. To be included in the study, at least two repeated diagnostic tests should have been conducted within 48-hour-intervals to arrive at a definitive diagnosis.

2.3. Image acquisition

All the patients who were hospitalized had undergone serial CXR. Posterior-anterior CXR scans were obtained with a digital radiography system (Revolution XQi ADS 28.4, GE Medical Systems, Milwaukee, WI, USA) and by adopting 70–120 kVp, 2–3 mA s and 180 cm source to

image distance. Portable digital radiography (MobileDaRt Evolution, Shimadzu, Kyoto, Japan) at bedside with anteroposterior projection was performed for patients who could not stand or move (by adopting 65–75 kV, 1.8–3.2 mA s, 100 cm source to image distance). The images were then interfaced directly to a picture archiving and communication system (Centricity 3.0; GE Healthcare, Mt. Prospect, IL, USA), which displayed all image data on two monitors (1536 × 2048 matrix, 10-bit viewable gray scale, and 450 cd per square meter).

2.4. Image analysis

Two chest radiologists assessed the CXRs (with 5 and 22 years of experience in chest imaging interpretation, respectively). They were blinded to patient information or disease progress, except for the knowledge that these were cases of MERS-CoV infection.

The extent of involvement on CXR was assessed independently for each of the 3 zones: upper (above the carina), middle (upper half of the craniocaudal distance of the remaining lung), and lower (lower half of the craniocaudal distance of the remaining lung) lung zones. The parenchymal abnormality on CXR was graded on a 3-point scale: 1, normal attenuation; 2, ground-glass attenuation; and 3, consolidation. The ground-glass opacity was defined as an area of hazy increased lung opacity, within which margins of pulmonary vessels may be indistinct [11]. Consolidation appears as a homogeneous increase in pulmonary parenchymal attenuation that obscures the margins of vessels and airway walls [11]. Each lung zone, with a total of six lung zones, was then graded based on the following scale (according to the area of the lung affected): 0 if normal, 1 if less than 25% of abnormality, 2 if 25–50% abnormality, 3 if 50–75% abnormality, and 4 if > 75% abnormality was noted. The four-point scale of the lung involvement was then multiplied by the 3-point scale of parenchymal abnormality in each lung zone, resulting in points ranging from 0 to 12 [12,13]. Points from all zones were added to arrive at a final total cumulative score, with values ranging from 0 to 72 (Fig. 1).

Presence of pleural effusion, laterality (unilateral vs. bilateral) of the lesions and that of fibrosing sequelae on serial CXR were also recorded. In terms of anatomic location, the distribution of parenchymal abnormalities was classified as central, peripheral, or mixed. The outer half of the lung was defined as peripheral, while the inner half was defined as central.

2.5. Statistical analysis

Statistical analysis was executed using SAS Version 9.4 (SAS Institute Inc, Cary, NC, USA). Differences in the clinico-radiological characteristics of the patients who were eventually intubated (intubation group) and those who were not (non-intubation group) were assessed using the Mann-Whitney U test for continuous variables and Fisher's exact test for categorical variables. Receiver operating characteristic (ROC) curve was plotted to select the appropriate cutoff value of radiographic score from day 5 to 18 to assess maximum sensitivity and specificity for fatal outcome. Univariate and multivariate logistic regression analyses were used to assess significant predictive factors for intubation. When everyday radiographic score was not available, a 3-day moving average of radiographic scores was applied. Interobserver agreements for radiographic scores were determined with intraclass correlation coefficients. $p < 0.05$ was considered to indicate a significant difference.

3. Results

3.1. Demographics and clinical characteristics

Detailed patient characteristics are shown in Table 1. Among 35 patients (22 men, 13 women; median age, 48 years) with laboratory confirmed MERS-CoV infection, 10 did not have any radiographic

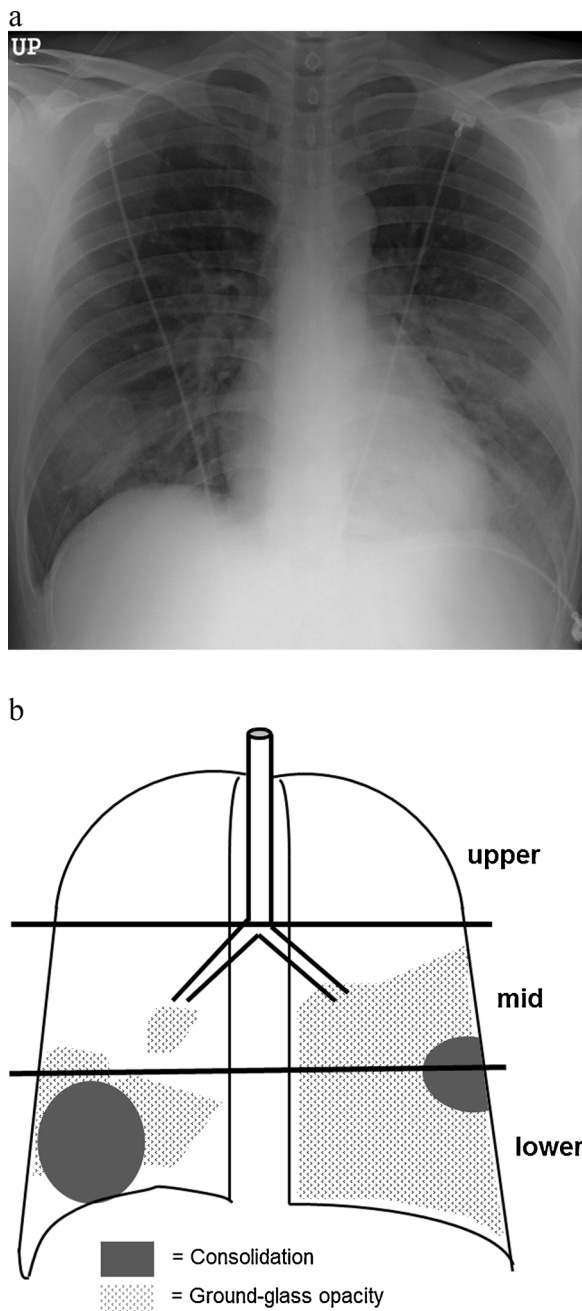


Fig. 1. Schematic diagram of radiographic scoring system. (a) Chest radiograph of a patient with MERS-CoV infection. (b) Schematic presentation of the extent of ground-glass opacity (GGO) and consolidation demonstrates a total score of 32, calculated as $2 \text{ (GGO)} \times 1$ ($\leq 25\%$ distribution in middle zone of the right lung) + $3 \text{ (consolidation)} \times 2$ (25%–50% distribution in lower zone of the right lung) + $2 \text{ (GGO)} \times 2$ (25%–50% distribution in lower zone of the right lung) + $2 \text{ (GGO)} \times 3$ (50%–75% distribution in middle zone of the left lung) + $3 \text{ (consolidation)} \times 1$ ($\leq 25\%$ distribution in middle zone of the left lung) + $3 \text{ (consolidation)} \times 1$ ($\leq 25\%$ distribution in lower zone of the left lung) + $2 \text{ (GGO)} \times 4$ (over 75% distribution in lower zone of the left lung).

abnormality and were categorized as MERS of upper respiratory tract infection (MERS URI). The remaining 25 patients with abnormality on CXR were classified as MERS pneumonia cases. Among the 25 patients with MERS pneumonia (15 men, 10 women; median age, 55 years), 18 were discharged without respiratory distress, whereas seven experienced fatal disease necessitating intubation or tracheostomy. The average time to intubation in these patients was 14 days [standard deviation (SD), ± 3.1]. Three of them eventually expired.

All patients were considered as tertiary (history of direct contact with secondary cases) cases of MERS. In terms of pre-morbid condition, no patient with MERS URI had an underlying disease, whereas seven patients (28%) with MERS pneumonia had underlying co-morbidities, such as diabetes mellitus ($n = 1$), chronic renal disease ($n = 1$), myelodysplastic syndrome ($n = 1$), ovarian cancer ($n = 1$), and colonic fistula ($n = 1$), or were older than 80 years ($n = 2$). On initial presentation, most patients complained of fever ($n = 34$), followed by myalgia ($n = 17$), respiratory symptoms such as cough, sputum and dyspnea ($n = 14$), gastrointestinal (GI) symptoms such as nausea, vomiting, and diarrhea ($n = 3$). The average time to symptom commencement from the virus exposure was 5.4 days (SD, ± 2.8 ; range, 2–11 days). The laboratory confirmation of MERS was obtained after an average of 9.3 days from the exposure (SD, ± 3.0 ; range, 5–15 days).

There was no significant difference between the intubation and non-intubation groups in terms of patients' demographics and clinical characteristics among patients with MERS pneumonia ($p > 0.05$), except for symptom presentation. Presence of respiratory symptom at initial presentation was significantly more common ($p = 0.030$), while presence of myalgia was significantly less common ($p = 0.030$), in the intubation group, compared with its counterpart (Table 1).

3.2. Radiographic findings

The average time from virus exposure to radiographic abnormality in 25 patients with MERS pneumonia was 9.2 days (SD, ± 2.8 ; range 5–15 days). In terms of distribution of parenchymal abnormalities, peripheral opacity was noted in 15 patients (60%), while diffuse involvement and central opacity was noted in 9 (37%) and 1 patient (4%), respectively. Bilateral lung involvement was noted in 16 patients (64%). Remaining opacity, categorized as fibrosing sequelae, was noted on serial CXRs in 13 patients (52%). Further, pleural effusion was noted in 14 patients (56%) and pneumothorax in one (4%).

Comparison of radiographic findings between intubation and non-intubation groups in patients of MERS pneumonia is summarized in Table 2. Peak radiographic score was significantly higher in intubation group, compared with non-intubation group ($p = 0.006$). It also revealed significantly higher diffuse lung involvement in intubation group, while peripheral lung involvement was more common in non-intubation group ($p = 0.003$). Additionally, all patients of intubation group demonstrated fibrosing sequelae on serial CXRs, whereas only 33% of the patients in non-intubation group showed remaining opacity ($p = 0.005$) (Fig. 2).

3.3. Radiographic score of 10 on day 10 as prognostic indicator

The sequential radiographic scores of patients with MERS pneumonia, classified as intubation and non-intubation groups are enumerated in Fig. 3. To obtain the cutoff value of radiographic score for the prediction of fatal outcome, we performed ROC analysis and the area under the ROC curve (AUC) of day 9 and day 10 achieved the best discriminatory performance (0.738 for day 9 and 0.726 for day 10) for the prediction of intubation. Table 3 shows the results of ROC analysis for the selection of cutoff radiographic score. The optimal cutoff radiographic score on day 9 was 6 with a sensitivity of 57.1%, specificity of 88.9% and Yonden's index of 0.460. The ROC analysis of day 10 demonstrated that an optimal cutoff value of radiographic score was 10 with a sensitivity of 57.1%, a specificity of 94.4%, Yonden's index of 0.516.

3.4. Logistic regression for the prediction of intubation

The results of univariate and multivariate logistic regression analyses for the prediction of respiratory distress have been enumerated in Table 4. Univariate analysis revealed that radiographic score ≥ 10 on day 10 significantly correlated with respiratory distress necessitating

Table 1
Baseline characteristics of Patients with MERS.

Characteristics	MERS URI (n = 10)	MERS Pneumonia			P value*
		All (n = 25)	Non-intubated (n = 18)	Intubated (n = 7)	
Age (yr) [†]	40.5 ± 17.6	53.2 ± 15.5	51.3 ± 13.3	57.9 ± 20.6	0.586
Sex (%)					0.179
Male	7 (70)	15 (60)	9 (50)	6 (86)	
Female	3 (30)	10 (40)	9 (50)	1 (14)	
Premorbid conditions (%)					0.066
No	10 (100)	18 (72)	15 (83)	3 (43)	
Yes	0 (0)	7 (28)	3 (17)	4 (57)	
Time to Symptom onset (day) [†]	6.9 ± 3.1	4.8 ± 2.5	5.0 ± 2.8	4.3 ± 1.6	0.878
Symptoms (%)					
Fever	10 (100)	24 (96)	17 (95)	7 (100)	0.999
Respiratory symptom	2 (20)	12 (48)	6 (47)	6 (86)	0.030
Myalgia	4 (40)	13 (52)	12 (67)	1 (14)	0.030
GI symptom	1 (10)	2 (8)	2 (11)	0 (0)	0.998
Time to RG abnormality (day) [†]	N/A	9.2 ± 2.8	9.6 ± 2.5	8.4 ± 3.5	0.295

Note: * P value was obtained in the comparison between intubated and non-intubated groups of MERS pneumonia. [†] mean ± standard deviation MERS = Middle East respiratory syndrome, URI = upper respiratory tract infection, GI = gastrointestinal, RG = radiographic.

Table 2
Comparison of radiological characteristics between intubated and non-intubated groups of MERS pneumonia.

Characteristics	MERS Pneumonia			P value*
	All (n = 25)	Non-intubated (n = 18)	Intubated (n = 7)	
Time to RG abnormality (day) [†]	9.2 ± 2.8	9.6 ± 2.5	8.4 ± 3.5	0.295
First RG score [†]	5.96 ± 4.28	5.17 ± 2.62	8.00 ± 6.86	0.442
RG score on the day of symptom onset [†]	0.38 ± 1.90	0	1.36 ± 3.59	0.143
Peak RG score [†]	25.80 ± 17.79	19.00 ± 13.09	43.29 ± 16.88	0.006
Distribution				0.071
Upper	3 (12)	2 (11)	1 (14)	
Lower	12 (48)	11 (61)	1 (14)	
Diffuse	10 (40)	5 (28)	5 (72)	
Location				0.003
Central	1 (4)	1 (6)	0 (0)	
Peripheral	15 (60)	14 (78)	1 (14)	
Diffuse	9 (36)	3 (16)	6 (86)	
Laterality				0.355
Unilateral	9 (36)	8 (44)	1 (14)	
Bilateral	16 (64)	10 (56)	6 (86)	
Fibrosing sequela	13 (52)	6 (33)	7 (100)	0.005
Pleural effusion	14 (56)	9 (50)	5 (71)	0.109
Pneumothorax	1 (4)	0 (0)	1 (14)	N/A

Note. [†] mean ± standard deviation MERS = middle east respiratory syndrome, RG = radiographic, N/A = not applicable.

intubation or tracheostomy [odds ratio (OR), 15.00; 95% confidence interval (CI), 2.01–191.22; $p = 0.023$]. Respiratory symptoms and absence of myalgia on initial presentation also showed significant correlation with respiratory failure ($P = 0.047$ and $= 0.047$, respectively). Variables with $p < 0.05$ on univariate analysis were used as the input variables for the multivariate analysis. Stepwise multivariate regression analysis demonstrated that radiographic score ≥ 10 on day 10 had the largest predictive power for respiratory failure, though not statistically significant (OR, 9.98; 95% CI, 0.875–196.35; $p = 0.097$).

3.5. Inter-observer agreement of radiographic scores

The inter-observer agreements between the two readers for the

calculation of radiographic scores were excellent with an ICC of 0.987 (95% CI, 0.982–0.991; $p < 0.001$).

4. Discussion

Our study demonstrated that a radiographic score ≥ 10 on day 10 from viral exposure is a parameter for the prediction of fatal disease course, which eventually necessitates invasive ventilator support. Several studies have discussed the imaging findings of MERS pneumonia. However, most of them focus on the CT findings rather than CXR [1,14]. Despite the availability of high resolution CT images, CXR is still the most important and commonly used modality in diagnosis and monitoring of highly contagious diseases such as MERS. Our study highlights the clinical implication of radiographic scores as a prognostic indicator in patients with MERS. As the average time to radiographic abnormality was 9.2 days (SD, 2.8 days) from viral exposure, prompt detection of CXR abnormality and acquisition of radiographic score is vital in the management of patients with MERS pneumonia.

Das et al. [15] also have reported about the clinical impact of chest radiographic score as an independent predictor of mortality in patients with MERS. One of unique findings of our study is that we identified the optimal time point and cutoff radiographic scores in patients with MERS pneumonia which could be used as an indicator of respiratory distress. In addition, our study demonstrated that patients' age and comorbidity did not differ significantly between intubation and non-intubation groups in patients with MERS pneumonia. These results are in contrast with the previous reports, including one by Das et al., which suggested that geriatric immunocompromised patients with MERS are at higher risk of fatal outcomes [15–18]. We found out that development of MERS pneumonia, rather than final outcome, was more frequently noted in patients with comorbidities. Indeed, none of the patients with MERS URI had premorbid conditions. We think that it can explain one of the mechanisms that patient's comorbidities had finally led to poor prognosis in previous reports. Current study emphasizes the importance of careful CXR monitoring in patients with MERS-CoV infection, regardless of patients' age and premorbid conditions.

One of the unique issues of Korean MERS outbreak is the so-called, super-spreaders, who resulted in extremely high human-to-human transmission rate. A total of 136 cases (73.1%) among 186 MERS patients of Korean outbreak, were actually transmitted from only three patients [8,18]. A recent report by Ko et al., specified the presence of radiographic abnormality, indicating MERS pneumonia in all three patients suspected of super spreading the infection [18]. Therefore, careful evaluation of CXR for detecting pneumonia is critical in the

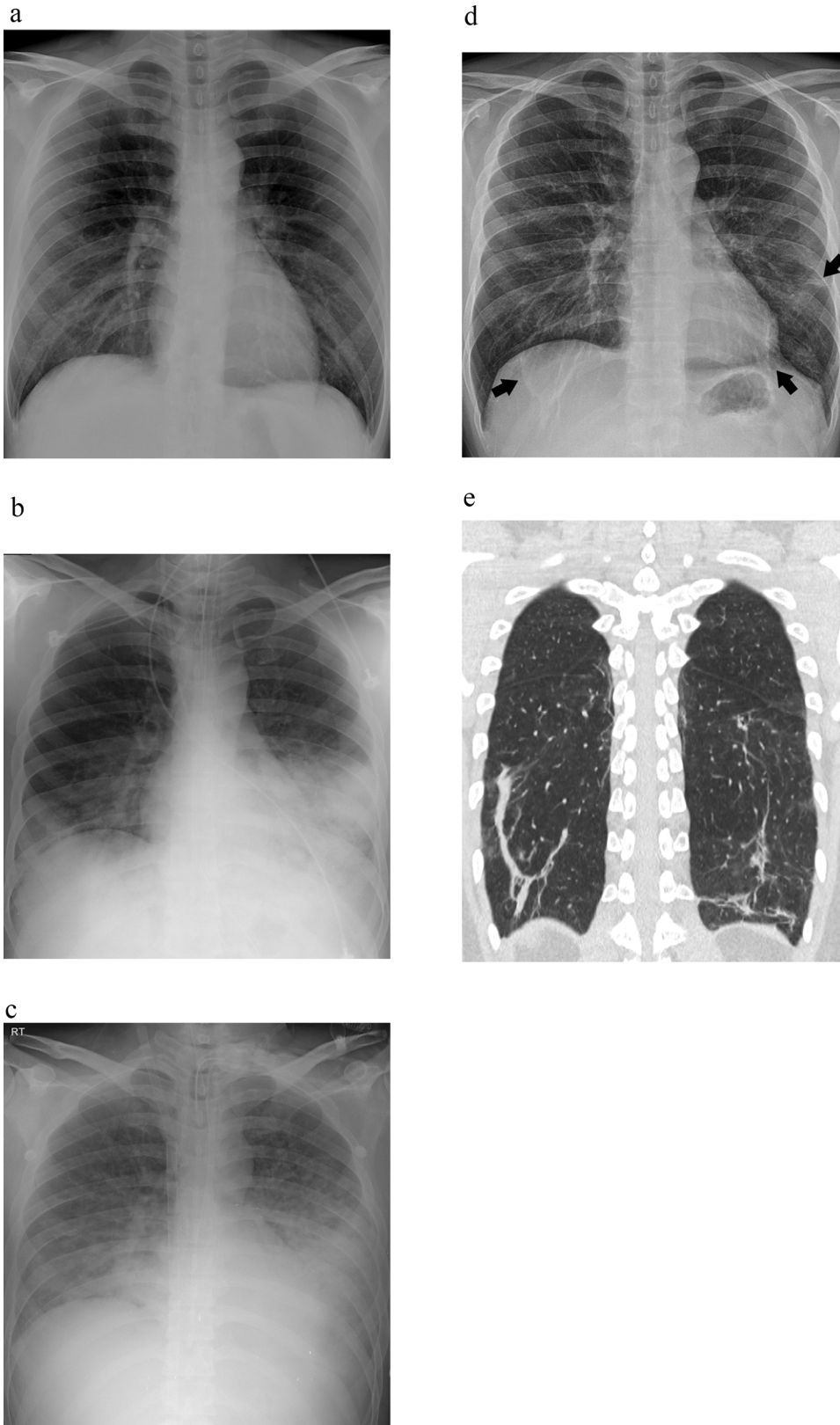


Fig. 2. A 32-year-old immunocompetent man with MERS-CoV infection. (a) Chest radiography (CXR) scan obtained on the day of symptom commencement (Day 4) is normal. (b) CXR scan obtained on Day 10 shows parenchymal opacity in bilateral middle and lower lung zones. The radiographic score is 24 and the patient is intubated. (c) CXR scan on Day 20 demonstrates increased area and density of parenchymal opacity with radiographic score of 36. (d) CXR scan obtained on Day 50 after discharge demonstrates remained linear or patchy opacities in both lungs (arrows), which may be fibrosing sequela. (e) The lesions correlate well with the CT scan.

control of MERS outbreak. Additionally, prediction of respiratory failure is also important to avoid urgent intubation or tracheostomy, which can increase the risk of transmission to healthcare workers. The average incubation period of MERS was estimated to be about 5.4 days, and could extend up to 11 days. The results of the current study support the efficacy of two-week quarantine system in patients with virus

exposure [19].

All of the patients of intubation group in our study showed remaining opacity as fibrosing sequela on follow-up CXR. Ajlan et al. [1] described the organizing pneumonia pattern of MERS pneumonia, with predominance of airspace opacities in the subpleural and basilar lung regions. In addition, Kim et al. recently reported a case of treated

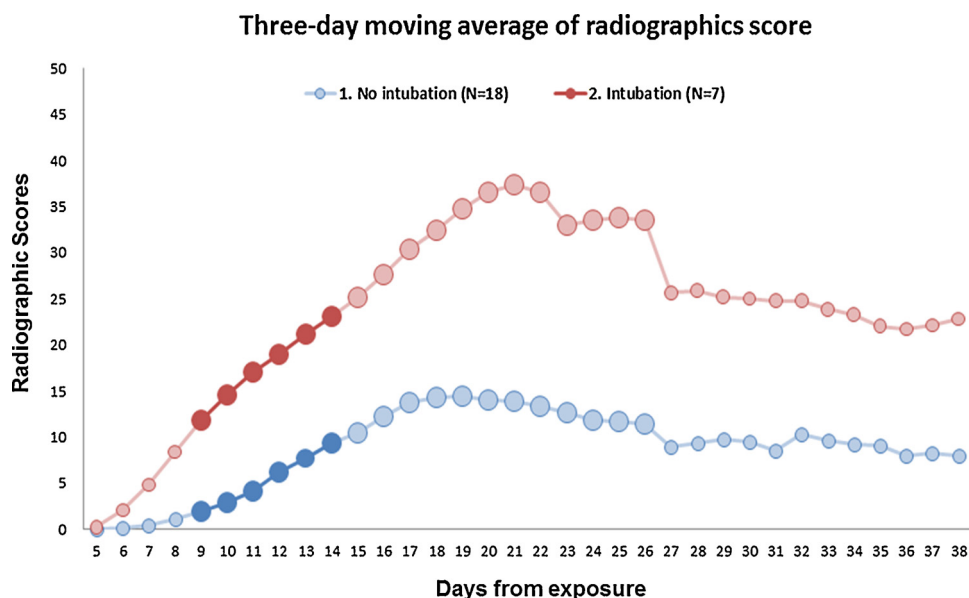


Fig. 3. Sequential radiographic scores of patients with MERS pneumonia. Curves show the difference in radiographic scores between patients with fatal cases of MERS versus patients who recovered without respiratory distress. Considering its maximal sensitivity and specificity, radiographic score of 10 on 10th day from viral exposure was considered as the optimal cutoff for prediction of respiratory distress.

Table 3
Cutoff Selection of Radiographic Scores on Day 9 and 10.

	Score	Accuracy	Sensitivity	Specificity	Yonden's Index	PPV ^f	NPV [§]
Day 9	2.7	64%	57.1%	66.7%	0.238	40%	80%
	4.3	72%	57.1%	77.8%	0.349	50%	82%
	6	80%	57.1%	88.9%	0.460	67%	84%
	17.8	84%	42.9%	100%	0.429	100%	82%
	29	76%	14.3%	100%	0.143	100%	75%
Day 10	2	60%	71.4%	55.6%	0.27	39%	82%
	3.4	64%	57.1%	66.7%	0.238	40%	80%
	6	72%	57.1%	77.8%	0.349	50%	82%
	7	80%	57.1%	88.9%	0.46	67%	84%
	10	84%	57.1%	94.4%	0.516	80%	85%
	24.7	84%	42.9%	100%	0.429	100%	82%
	34.7	76%	14.3%	100%	0.143	100%	75%

Note. ^fPPV = Positive predictive value, [§]NPV = Negative predictive value. Bold values indicate the optimal cutoff radiographic score on day 9 and day 10, showing maximum sum of sensitivity and specificity.

Table 4
Univariate and Multivariable Analysis for the Prediction of Intubation.

Univariate Analysis			
Variables	Crude Odds Ratio	95% Confidence Interval	p Value
Sex, female	0.23	0.0–1.4	0.167
Premorbid conditions	5.7	1.0–39.5	0.074
Respiratory Symptoms	8.33	1.3–93.6	0.047
Myalgia	0.12	0.0–0.7	0.047
RG score on Day 10, ≥ 10	15.00	2.01–191.22	0.023
Multivariate Analysis using Stepwise Selection			
Variables	Adjusted Odds Ratio	95% Confidence Interval	p Value
RG score on Day 10, ≥ 10	9.98	0.875–196.35	0.097

Note. Bold, $p < 0.05$.

organizing pneumonia in patient with MERS-CoV infection [20]. We can assume that fibrotic changes leaving linear or patchy opacities on follow up CXRs may have resulted from organizing pneumonia. Further studies are required to identify the radiological and pathological

evolution of MERS pneumonia.

There were several limitations in this study. First, it was a retrospective study and might have limited power in identifying prognostic factors. Second, although the radiographic score ≥ 10 on day 10 had the largest predictive power for respiratory failure, it was not found to be statistically significant on multivariate analysis. We think that a small number of study population was a major drawback of our result, which hindered statistical significance. As there is limited number of patients with MERS, we hope that external validation of our radiographic scoring system would be performed by other MERS-CoV research group to establish a role of radiographic score as a prognostic indicator in MERS pneumonia. Third, daily CXRs were not available in most cases, as CXR scans were obtained on every other day in the recovery phase. To overcome the issue, we applied 3-day moving average value of radiographic scores to minimize the potential error. Lastly, the sensitivity, specificity and AUC of radiographic score might not be sufficiently high enough. We admit that CXR may not be the most efficient diagnostic or prognostic tool for patients with MERS. However, we should not overlook the clinical utility of CXR as an indispensable modality for patients with this highly contagious disease.

In conclusion, MERS has threatened the public health not only with its high transmission rate, but also with high fatality and mortality. We suggest that radiographic scores can play a vital role in the management of patients with MERS because of the ability to predict respiratory distress necessitating ventilator support. Patients with radiographic score ≥ 10 on day 10 from viral exposure are in need of aggressive therapy with careful surveillance and follow-up evaluation.

Declarations of interest

None.

Acknowledgements

We express our sincerest condolences to the patients and family members who suffered from the MERS outbreak. We also appreciate the health care personnels at Samsung Medical Center and all other hospitals who worked together to overcome the MERS outbreak in Korea.

References

[1] A.M. Ajlan, R.A. Ahyad, L.G. Jamjoom, A. Alharthy, T.A. Madani, Middle East respiratory syndrome coronavirus (MERS-CoV) infection: chest CT findings, *AJR Am.*

- J. Roentgenol. 203 (4) (2014) 782–787.
- [2] A.M. Zaki, S. van Boheemen, T.M. Bestebroer, A.D. Osterhaus, R.A. Fouchier, Isolation of a novel coronavirus from a man with pneumonia in Saudi Arabia, *N. Engl. J. Med.* 367 (19) (2012) 1814–1820.
- [3] W.H. Organization, Middle East Respiratory Syndrome Coronavirus (MERS-CoV), (2017) <http://www.who.int/emergencies/mers-cov/en/>.
- [4] Korea Ministry of Health and Welfare KCfDCaP, Summary of MERS Statistics in the Republic of Korea, (2015) http://www.mers.go.kr/mers/html/jsp/Menu_C/list_C4.jsp.
- [5] M.M. Al-Abdallat, D.C. Payne, S. Alqasrawi, et al., Hospital-associated outbreak of Middle East respiratory syndrome coronavirus: a serologic, epidemiologic, and clinical description, *Clin. Infect. Dis.* 59 (9) (2014) 1225–1233.
- [6] A. Assiri, A. McGeer, T.M. Perl, et al., Hospital outbreak of Middle East respiratory syndrome coronavirus, *N. Engl. J. Med.* 369 (5) (2013) 407–416.
- [7] I.K. Oboho, S.M. Tomczyk, A.M. Al-Asmari, et al., 2014 MERS-CoV outbreak in Jeddah—a link to health care facilities, *N. Engl. J. Med.* 372 (9) (2015) 846–854.
- [8] S.Y. Cho, J.M. Kang, Y.E. Ha, et al., MERS-CoV outbreak following a single patient exposure in an emergency room in South Korea: an epidemiological outbreak study, *Lancet* 388 (10048) (2016) 994–1001.
- [9] J.A. Al-Tawfiq, Z.A. Memish, Managing MERS-CoV in the healthcare setting, *Hosp. Pract.* (1995) 43 (3) (2015) 158–163.
- [10] J.H. Lee, C.S. Lee, H.B. Lee, An appropriate Lower respiratory tract specimen is essential for diagnosis of Middle East Respiratory Syndrome (MERS), *J. Korean Med. Sci.* 30 (8) (2015) 1207–1208.
- [11] D.M. Hansell, A.A. Bankier, H. MacMahon, T.C. McLoud, N.L. Muller, J. Remy, Fleischner Society: glossary of terms for thoracic imaging, *Radiology* 246 (3) (2008) 697–722.
- [12] F. Feng, Y. Jiang, M. Yuan, et al., Association of radiologic findings with mortality in patients with avian influenza H7N9 pneumonia, *PLoS One* 9 (4) (2014) e93885.
- [13] K.T. Wong, G.E. Antonio, D.S. Hui, et al., Severe acute respiratory syndrome: radiographic appearances and pattern of progression in 138 patients, *Radiology* 228 (2) (2003) 401–406.
- [14] K.M. Das, E.Y. Lee, M.A. Enani, et al., CT correlation with outcomes in 15 patients with acute Middle East respiratory syndrome coronavirus, *AJR Am. J. Roentgenol.* 204 (4) (2015) 736–742.
- [15] K.M. Das, E.Y. Lee, S.E. Al Jawder, et al., Acute Middle East respiratory syndrome coronavirus: temporal lung changes observed on the chest radiographs of 55 patients, *AJR Am. J. Roentgenol.* 205 (3) (2015) W267–W274.
- [16] D.S. Hui, Z.A. Memish, A. Zumla, Severe acute respiratory syndrome vs. The Middle East respiratory syndrome, *Curr. Opin. Pulm. Med.* 20 (3) (2014) 233–241.
- [17] A. Zumla, D.S. Hui, S. Perlman, Middle East respiratory syndrome, *Lancet* 386 (9997) (2015) 995–1007.
- [18] J.H. Ko, G.E. Park, J.Y. Lee, et al., Predictive factors for pneumonia development and progression to respiratory failure in MERS-CoV infected patients, *J. Infect.* 73 (5) (2016) 468–475.
- [19] A. Assiri, J.A. Al-Tawfiq, A.A. Al-Rabeeah, et al., Epidemiological, demographic, and clinical characteristics of 47 cases of Middle East respiratory syndrome coronavirus disease from Saudi Arabia: a descriptive study, *Lancet Infect. Dis.* 13 (9) (2013) 752–761.
- [20] I. Kim, J.E. Lee, K.H. Kim, S. Lee, K. Lee, J.H. Mok, Successful treatment of suspected organizing pneumonia in a patient with Middle East respiratory syndrome coronavirus infection: a case report, *J. Thorac. Dis.* 8 (10) (2016) E1190–E1194.